ELSEVIER

Journal of Structural Geology 29 (2007) 1900–1914

JOURNAL OF STRUCTURAL GEOLOGY

www.elsevier.com/locate/jsg

Antithetic fault linkages in a deep water fold and thrust belt

Simon Higgins [a,*], Richard J. Davies [b], Benjamin Clarke [c]

[a] 3DLab, School of Earth, Ocean and Planetary Sciences, Main Building, Park Place, Cardiff University, Cardiff, CF10 3YE, UK
[b] CeREES, (Centre for Research into Earth Energy Systems) Department of Earth Sciences, University of Durham, Science Labs, Durham DH1 3LE, UK
[c] Statoil asa (Global Exploration), 4035 Stavanger, Norway

Received 9 March 2007; received in revised form 11 September 2007; accepted 12 September 2007
Available online 31 October 2007

Abstract

Deep water fold and thrust belts consist of both forethrusts and backthrusts that can link along strike to form continuous folds in the overburden. The interaction of faults of opposing dip are termed 'antithetic thrust fault linkages' and share the common feature of a switch in vergence of overlying hangingwall anticlines. Using three-dimensional seismic data, on the toe-of-slope of the Niger Delta, linkages are classified into three distinct structural styles. This preliminary classification is based on the vertical extent of faulting within a transfer zones relative to the branch line of the antithetic faults. The stratigraphic level of the lateral tip of the fault, the shape of lateral tip region of a fault plane and the stratal deformation within the transfer zones is also distinctive in each type of fault linkage. A Type 1 linkage comprises faults that overlap exclusively above the level of the branch line. A 'pop-up' structure forms within the transfer zone with sediments below remaining planar. The lower tip lines of faults climb stratigraphically towards the linkage zone creating asymmetric, upward-tapering lateral tip regions. In Type 2 linkages fault overlap occurs lower than the level of the branch line such that lateral fault tips are located within the footwall of the counterpart fault. Faulting is thus limited to the deeper section within the transfer zone and creates unfaulted, symmetric, bell-shaped folds in the overburden. Upper tip lines of faults lose elevation within the transfer zone creating asymmetric, downwards-tapering lateral tip regions. In Type 3 linkages both faults continue above and below the branch line within the transfer zone resulting in cross-cutting fault relationships. Horizon continuity across the folds, through the transfer zones, varies significantly with depth and with the type of fault intersection.

Keywords: Thrust faults; Fault linkage; Antithetic; Transfer zones; Vergence

1. Introduction

Research into the growth, propagation and linkage of faults has predominantly focused upon extensional rather than reverse displacement. Numerous studies on extensional faults have provided insights into along strike and down-dip displacement variations (e.g. Peacock and Sanderson, 1991), fault growth (e.g. Watterson, 1986; Barnett et al., 1987; Cartwright et al., 1995), fault scaling laws (e.g. Dawers and Anders, 1995), and classifications of fault linkage geometries (e.g. Gawthorpe and Hurst, 1993). Thrust faults are fundamental as a mechanism for accommodating shortening in convergent tectonic settings and in gravitational detachment systems. Despite this, the mechanisms by which thrusts initiate, propagate and link are not well defined. Most studies have focused on fault geometries, displacement variations and growth using dip-parallel outcrop exposures (e.g. Williams and Chapman, 1983; Eisenstadt and De Paor, 1987; Ellis and Dunlap, 1988). Analyses of along-strike variations and linkage are fewer (e.g. Dahlstrom, 1970; Aydin, 1988; Harrison and Bally, 1988; Nicol et al., 2002; Davis et al., 2005), possibly due to partial exposure and the preferential erosion of hangingwalls within ancient thrust systems (Davis et al., 2005). Analogue modelling of thrust systems provide useful indications as to how thrusts may initiate and grow by segment linkage (e.g. Liu and Dixon, 1991) but remain largely untested in the field. This paper describes and classifies along-strike linkages of

* Corresponding author. Tel.: +44 2920870010.
E-mail addresses: higginss1@cf.ac.uk (S. Higgins), richard.davies@durham.ac.uk (R.J. Davies), bjcl@statoil.com (B. Clarke).

0191-8141/$ - see front matter © 2007 Elsevier Ltd. All rights reserved.
doi:10.1016/j.jsg.2007.09.004

thrust faults of opposing dip and demonstrates an associated change in fold geometry. This is intended as a preliminary classification to form a basis for further research.

The acquisition of high resolution three-dimensional seismic data over deep water fold and thrust belts offers an opportunity to better resolve fault plane geometries and linkages in three-dimensions. We have selected the compressional domain of the deep water Niger Delta fold and thrust belt, as it provides first class examples of along-strike linkage of thrusts.

1.1. Along-strike thrust fault linkage

Thrust faults can link in the direction of strike such that displacement reduces to zero on one fault, whilst increasing in the same direction on the next (e.g. Davis et al., 2005) in a similar manner to extensional fault systems (Larsen, 1988). This can take place on faults that have similar or opposing direction of dip, termed synthetic and antithetic respectively (Peacock et al., 2000). The regions where fault displacement is transferred from one fault to the next are termed 'transfer zones' (Dahlstrom, 1970). Connectivity of thrusts through transfer zones is not a new concept (e.g. Douglas, 1958; Dahlstrom, 1970; Boyer and Elliot, 1982). Pfiffner (1985), for instance, described a decrease in master fault displacement by the ''consumption'' of slip by minor splays, whilst Dahlstrom (1970) illustrated the transfer of displacement between paired faults (and folds) along a through-going sole thrust. This led to a simple three-dimensional model of a synthetic transfer zone of en echelon thrust faults (Dahlstrom, 1970 their Figure 26).

Descriptions of antithetic interactions are less common and are largely contained within studies of triangle zones and descriptions of back thrust splays on larger synthetic 'master' faults (e.g. Mandl and Crans, 1981). McClay (1992) and Couzens and Wiltschko (1996) classify two types of triangle zone from existing literature; the first involving two thrusts detaching on a single decollement (Fig. 1a) and the second, also described as an intercutaneous wedge (McClay, 1992), containing multiple decollements (Fig. 1b). The first type can be described as a structure composed of two dipping reflections underlain by horizontal reflections (Couzens and Wiltschko, 1996) (Fig. 1a). Some interactions between faults in this study fulfill this criteria but, importantly, overlap both laterally and downdip within the transfer zone. Back thrust splays have less relevance to this study as they are not thought to be due to the interaction and linkage of two distinct, independent faults and may exist to accommodate strain induced in the hangingwall during ramp climb of the master fault (Butler, 1982).

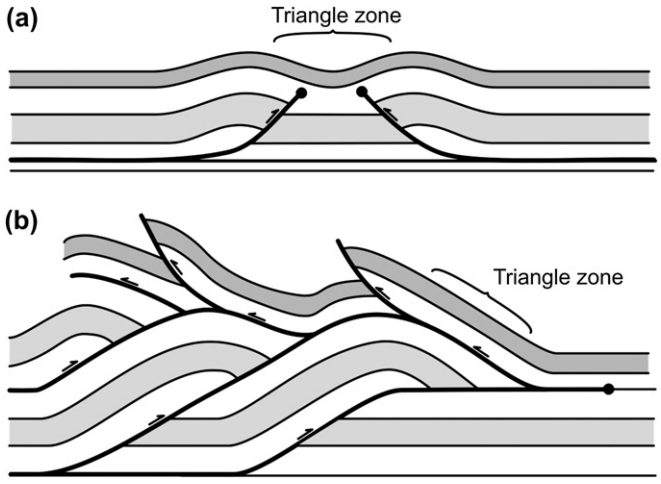

Fig. 1. Illustration of triangle zone geometries (from Couzens and Wiltschko, 1996). (a): ''Type I triangle zone'' (Couzens and Wiltschko, 1996). (b) Intercutaneous wedge (McClay, 1992) or ''Type II triangle zone'' (Couzens and Wiltschko, 1996).

The initiation and propagation of thrusts can lead to the development of an asymmetric hangingwall anticline ahead of the fault (e.g. Suppe, 1985 their Figure 9.47). Fig. 2 describes how this asymmetry can be given as a direction of fold vergence, defined here as being towards the shorter, commonly steeper limb from the axial surface. The most evident indication that thrust faults of opposing dip are linking along strike, within the subsurface, can be a switch in the direction of vergence of associated folds in the overburden (Fig. 2). These changes in vergence of hangingwall anticlines are common in the deep water Niger Delta and represent the interaction of detaching forethrusts and backthrusts in the underlying sediments. The seismic data used here contain examples of along-strike overlap and interaction of fault tip regions, although the considerable scale of the faults means it is uncommon for both ends of a particular fault to lie within data limits. Displacement transfer, indicated by horizon geometries, heave-length profiles and the complimentary shape of overlapping fault tip lines, implies kinematic interaction between all the fault pairs identified in this study (Huggins et al., 1995). As a result, the rock volume within a zone of geometric overlap between two fault tips is referred to here as a 'transfer zone' (Dahlstrom, 1970). The examples of transfer zones, imaged using three-dimensional seismic data, are classified into distinct structural styles and geometries.

2. Study area

The 3D seismic survey used in this study covers ~3000 km^2 of the compressional toe-of-slope fold and thrust belt of the Niger Delta. Inline and crossline spacing is 12.5 m (e.g. Brown, 1999) with vertical resolution varying from approximately 7.5 m in shallow levels to 20 m at the base of the studied interval. A review of the geology of the Niger Delta is provided by Doust and Omatsola (1990). Extension and contraction within the delta system is driven by large-scale gravitational collapse on regional detachment levels existing within the Akata Formation (e.g. Bilotti and Shaw, 2005) resulting in the downslope translation of the overlying Agbada Formation. Individual thrust faults have been documented as detaching at numerous levels within the succession of the Niger Delta (Corredor et al., 2005; Briggs et al., 2006). There are two detachments levels imaged in this data set; at the Agbada-Akata Formation boundary and a regional detachment within the Akata itself. Within the study area the Agbada Formation

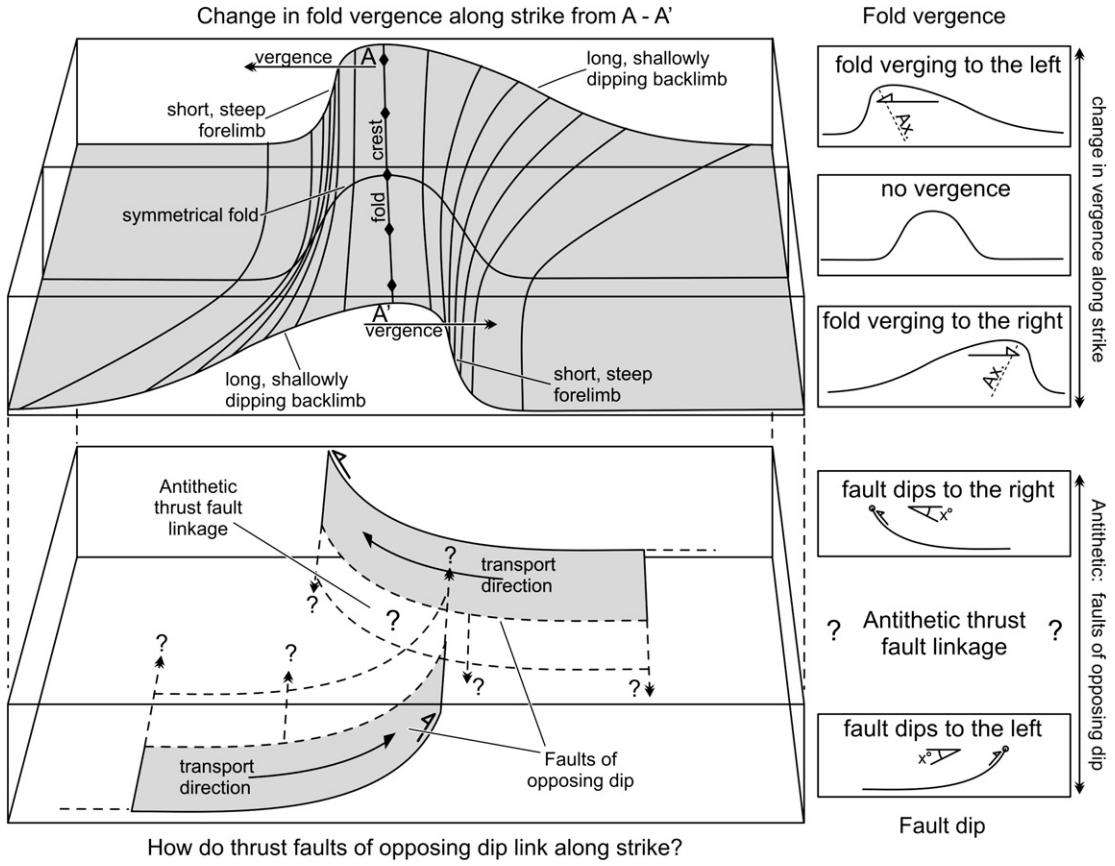

Fig. 2. Diagrammatical description of fold vergence reversal and antithetic thrust fault linkage. Thrust faults in the subsurface underlie asymmetric, verging anticlines. Vergence is defined as toward the shorter, steeper limb from the core of the fold. The upper block diagram shows a switch in the vergence of the fold along strike coinciding with an antithetic thrust fault linkage below. Antithetic linkage is defined as the interaction of faults with opposing dip. The geometry of the transfer zone between the two thrusts varies and is classified into three types in the text. Ax., axial plane.

comprises a series of stacked deepwater channel-levee systems (e.g. Deptuck et al., 2003) and is deformed into 21 large-scale, detaching oceanward-vergent forethrusts and landward-vergent backthrusts. The fold and thrust belt, if modelled as a critical taper wedge, has a relatively shallow bathymetric slope (Bilotti and Shaw, 2005) leading to the inference of a weak basal detachment. This causes the maximum principal compressive stress to be subhorizontal and close to the angle of the detachment. In such a scenario there is little mechanical advantage between the formation of a forethrust or a backthrust, which have similar dip angles and are equally efficient at accommodating shortening (Bilotti and Shaw, 2005). The focus of this paper surrounds the linkage of thrusts of opposing dip. We do not expect the predominance of antithetic linkage to be generic or universal; it simply indicates a difficulty in clearly imaging synthetic interactions, due in part to overprinting of displacement variations by well-developed, closely spaced, stacked forethrusts. Forethrust–forethrust interactions in this area are commonly characterised by a subtle bend in the fault trace and an along-strike displacement minimum. It is conceivable that if linkage between similarly dipping and laterally aligned faults occurred early in their history then signs of this mechanism may be lost at the resolution of seismic data.

3. Depth conversion

This paper describes the geometries of fold and thrust structures using 3D seismic data and two-way-travel time (twt) seismic sections. It is therefore important to establish the significance of any change to structural geometries that may occur during time to depth conversion (see Brown, 1999). Depth conversion was performed on all seismic sections used in the study using interval velocities from a nearby well. Fig. 3 shows two representative time sections (a and c) across two linkage zones and their depth converted equivalents (b and d). It is apparent that, in both cases, the shallow section (less than ~ 5 s and ~4 km) is relatively unchanged in thickness and geometry during the calculation. The deeper section however displays some dramatic thickening of the section, below 6 s and 5 km, due to an increase of velocity with depth. If one ignores the thickness changes, the (d) depth section is largely unchanged geometrically and is typical of the majority of sections in this data set. Depth conversion of the (a) time section, however, results in apparent symmetric folds (between 6 and 7 s) being transformed into planar dipping reflectors in the (b) depth section (Fig. 3). This is less common in this study and is due to velocity pull-up (see Brown, 1999) caused by the

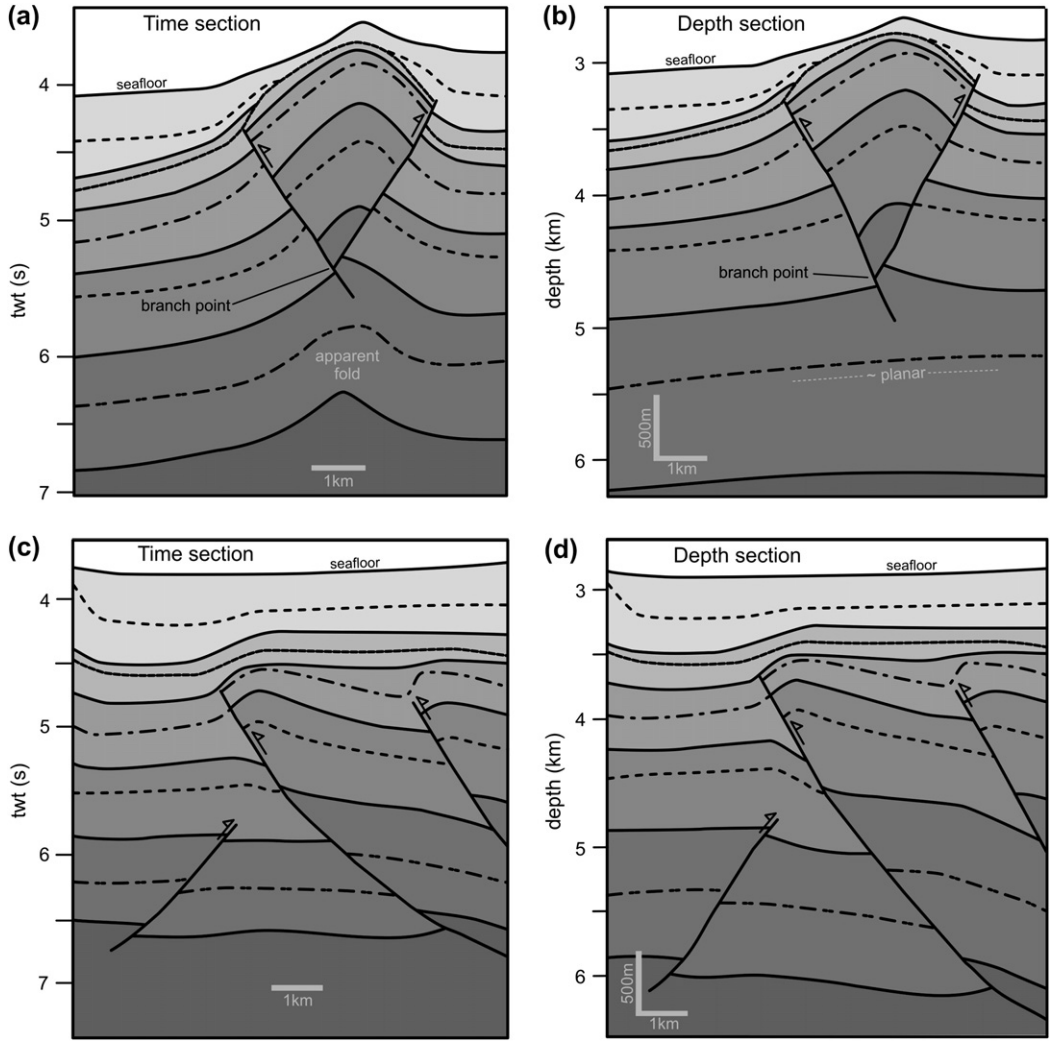

Fig. 3. Cross sections to show depth conversion of representative time sections. (a), (b) A section containing a pop-up structure in a Type 1 linkage. (c), (d) A section towards the lateral edge of a Type 2 linkage. Above 4 km (b and d) sections are relatively unchanged by depth conversion. Deeper than 4 km, there is significant thickening. In (a), symmetrical folds beneath the pop-up are transformed into planar, dipping reflectors during depth conversion (b). Geometrically (ignoring thickness changes) (c) resembles (d), even at depth.

seafloor expression of the overlying fold combined with the uplift of high velocity rocks within the pop-up structure.

Seismic time sections are therefore used to describe structural geometries herein as the large majority of time sections are not significantly altered during depth conversion (as in Fig. 3(c)–(d)). Exceptional velocity effects are referred to in the text.

4. Observations

4.1. Profile of a single fault and fold

Many studies of fault linkage within extensional settings use a single, isolated, blind normal fault as a reference standard from which to identify modifications to a fault profile due to interaction with a free surface, mechanical boundary, unconformity or neighbouring fault (e.g. Barnett et al., 1987; Walsh and Watterson, 1991; Huggins et al., 1995). In the Niger Delta, where faults are commonly longer than the extent of 3D datasets, there is a paucity of fully imaged, compressional faults. In addition to this, all faults observed in this structural domain either interact with another fault or detach at some point along their length and may, in the case of fault propagation folds, have nucleated in the decollement.

The simplest example of a fold and thrust from the Niger Delta dataset, and one that shows little evidence of having interacted with neighbouring structures, is described in Fig. 4. This structure is only partially imaged and extends approximately 25 km from the fault and fold tip to the data edge (Fig. 4a). The fault trace is somewhat arcuate in map view but shows no significant jogs that could indicate linkage (e.g. Cartwright and Trudgill, 1994). The profiles of fault displacement and fold crest elevation increase similarly away from the tip of the structure and show no major changes in gradient along their length (Fig. 4b and c). The shape of the single fault plane within the fold (Fig. 4d and e) is used as a reference

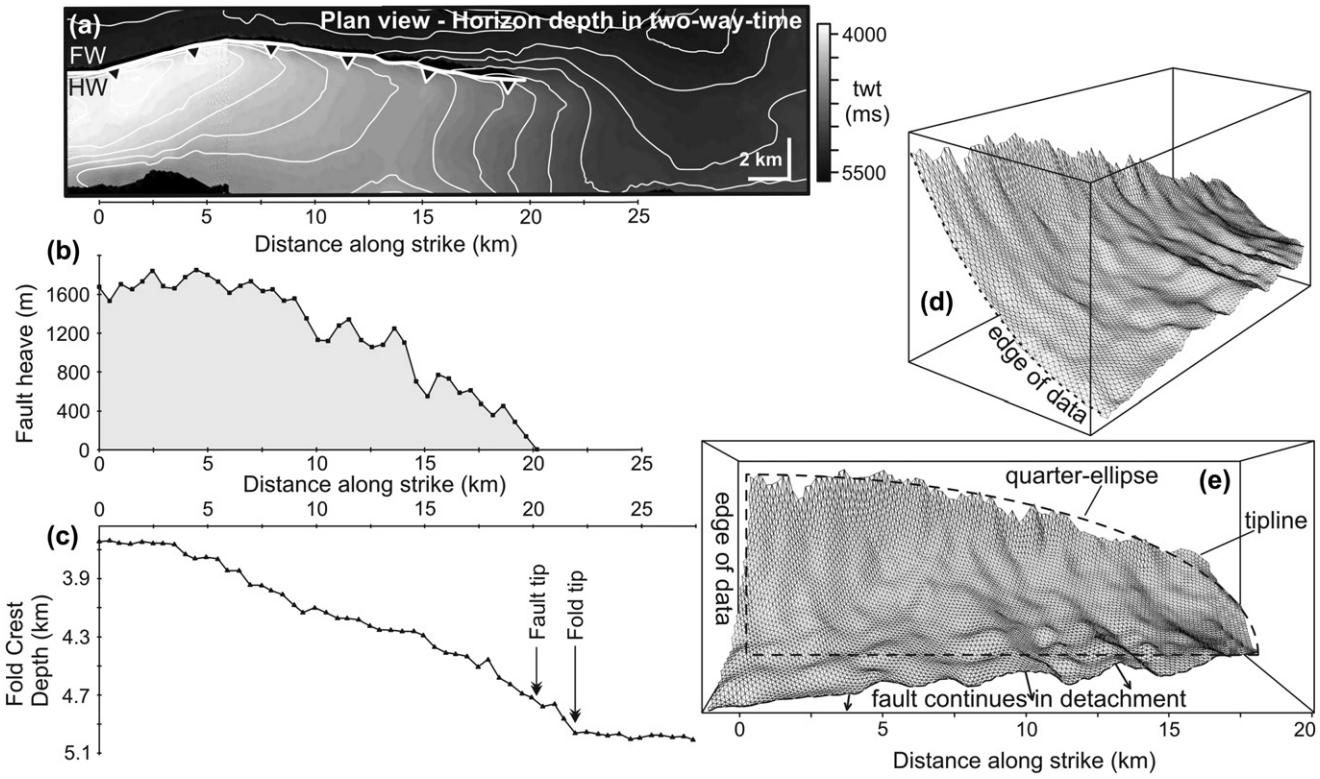

Fig. 4. Profile of a single fault and fold. (a) Map of a folded horizon given in two-way-time (ms). Dark greys represent structural lows, lighter greys are structural highs. FW, footwall; HW, hangingwall. (b) Heave-length plot for the selected horizon. (c) Fold elevation chart plotting depth to fold crest vs. distance along strike. (d) 3D visualisation of a gridded thrust fault surface. (e) 3D visualisation of a thrust surface looking down-dip to show the shape of the fault tipline.

when describing examples of antithetic linkage in this study. Of particular importance here is the shape of the lateral tip region of the fault expressed by the upper tipline, the upper edge of the gridded surface (Fig. 4d and e). Ideal isolated normal faults (Barnett et al., 1987) are described as elliptical with a symmetric lateral taper, such that upper and lower tiplines converge equally towards a central lateral fault tip. In the case of this detaching thrust (Fig. 4) a large part of the fault plane is hidden in a zone of bed parallel shear within the detachment, whilst a lateral portion is not imaged due to the location of the data limits. As a result it may be argued that as little as a quarter of the fault is observable. It is evident from the gridded surface of the single thrust (Fig. 4e) that the tipline decreases in elevation along strike towards the tip, whilst increasing in gradient, such that the shape of the fault plane resembles a quarter-ellipse (Fig. 4e). It is predicted that a complete, isolated fault would form a semi-ellipse, the chord of which would be located on the detachment. It is hypothesised that linking faults display modifications to this model that are characteristic of the type of linkage involved.

4.2. Antithetic linkage (forethrust to backthrust)

Antithetic transfer zones have a range of distinct structural geometries whilst all showing vergence reversals (the switching of vergence along strike) in associated folds (Fig. 5). The term ‘transfer zone’ is used to describe a region of displacement transfer between two interacting thrust faults. This can be demonstrated using displacement–length (d–x) profiles for each transfer zone that compare the magnitude of faulting on each constituent fault with distance along strike. Here, fault heave is used, as opposed to along-fault displacement (Fig. 6). Note the example profiles (Fig. 6) comprise measurements made on the faults corresponding to the folds of Fig. 5. Ideal, isolated faults are thought to have linear d–x profiles, from the point of maximum displacement (d_{MAX}) to the fault tip, approximating to the Walsh and Watterson (1987) cumulative slip profile (Peacock and Sanderson, 1991). Linking faults have been shown to display modifications to this model such that d–x profiles can consist of two straight portions, the first from d_{MAX} to the start of the relay and a second, steeper section, from the start of the relay to the fault tip (Peacock and Sanderson, 1991). The overlap of elastic strain fields during growth causes the slip distribution of a fault to be affected by the other (Segall and Pollard, 1980; Childs et al., 1995; Nicol et al., 1996). This can produce convex-up profiles resulting from an increase in displacement gradient towards the fault tips due to a retardation or arrest of lateral propagation and the transfer of displacement between linking structures. Overlapping faults that lack displacement transfer are therefore kinematically independent and are either too widely separated spatially or grew at different times. All faults described in this study exhibit abrupt increases in heave gradient towards the linkage zones and commonly have steeper profiles within the linkages than without (Fig. 6). The backthrust of the Type 2 example (Fig. 6b) is the exception as a significant

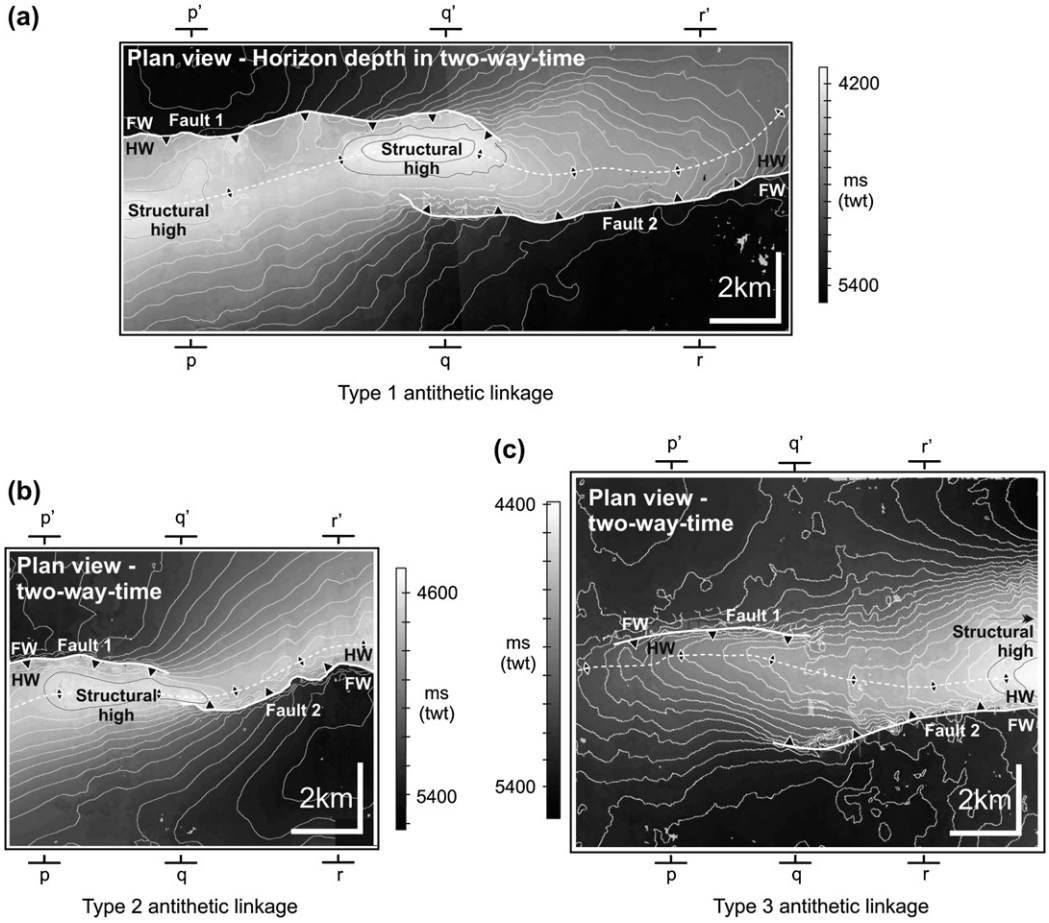

Fig. 5. Maps of a folded horizon for antithetic Types 1, 2 and 3 linkages given in two-way-time (ms) to demonstrate vergence reversals along strike. Dark greys represent structural lows, lighter greys are structural highs. FW, footwall; HW, hangingwall. Hinge lines are represented by a stippled white line and black diamonds. The hangingwall intersection with a fault is given by black triangles. (p–p', q–q', r–r') give the locations of seismic sections in Figs. 7, 9 and 10. The vergence of the fold can be determined to be towards the steeper limb from the fold crest as shown by the contours and shading. Note that structural highs occur close to the zone of overlap of the faults in Type 1 and 2 linkages. Also, the amount of overlap of the faults seen here only corresponds to this given horizon. For maximum fault overlap see later figures.

part of it not imaged beyond the edge of the data. The profiles of antithetic thrust fault linkages (Fig. 6) therefore indicate kinematic interaction during linkage and suggest fault pairs grew concomitantly.

These examples of kinematically linked, antithetic faults are used in this study to illustrate three subdivisions of thrust interaction based on fault plane geometries and horizon deformation that incorporate all permutations of linkage seen in this part of the Niger Delta.

4.2.1. Antithetic Type 1 linkage

This type of interaction is illustrated by the linkage of two thrusts which detach at similar levels (Fig. 7). The faults are spatially coincident within a single, 30 km long, continuous anticline that spans the hangingwalls. The fold switches vergence and is doubly-plunging with the culmination occurring above the mid-point of the transfer zone (Figs. 5 and 7b). Fold amplitude decreases to zero away from the linkage along strike in one direction, and remains relatively constant until meeting the data limit in the other. The interaction of these faults is illustrated using successive seismic sections across the fold (Fig. 7a, b and c) the locations of which are given in Fig. 5.

Relatively simple thrusted folds on either side of the transfer zone are contrasted with the structures within. Along strike of the zone of overlap a single backthrust (Fig. 7a) ramps upward from the detachment and has an approximate maximum along-fault displacement of 1.5 km (Fig. 7 p–p') measured on horizons immediately above the Agbada-Akata Fm boundary. The hangingwall anticline verges in the transport direction (to the right) with the shorter forelimb facing upslope and the longer, shallowly dipping backlimb facing downslope. The Agbada-Akata Fm boundary is offset and displays ‘apparent’ footwall folding caused by a velocity effect due in part to the seafloor expression of the fold (see below and Fig. 3).

This geometry is mirrored along strike, in the opposite direction from the transfer zone (Fig. 7c). An oceanward propagating forethrust, with approximately 1.3 km displacement in this section, produces an asymmetric hangingwall anticline that verges downslope (to the left, Fig. 7 r–r'). The Akata

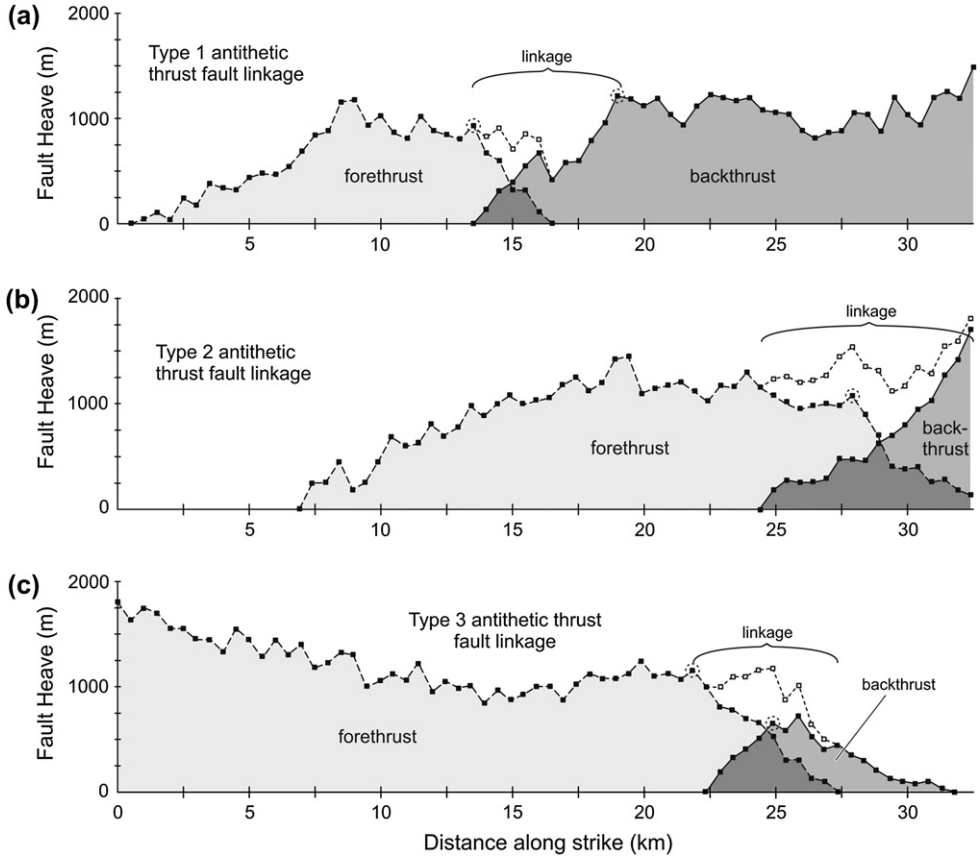

Fig. 6. Heave–distance plots for examples of Type 1–3 linkage. (a) Type 1 antithetic thrust fault linkage. Stippled circles indicate points of abrupt change in displacement gradient towards the linkages. (b) Type 2 antithetic thrust fault linkage. (c) Type 3 antithetic thrust fault linkage.

marker surface is again offset in a reverse sense, with 'apparent' folding (see below and Fig. 3) close to the fault plane in the footwall.

The transition along strike from forethrust to backthrust occurs within a transfer zone, the centre of which is shown in Fig. 7b (q–q'). Here the fold displays no vergence and two faults converge on a predicted point of intersection, or 'branch point' (e.g. McClay, 1992). A symmetrical fold in the shallower stratigraphy has equally dipping limbs and is bounded on both sides by faults in a 'pop-up' structure above the branch point. At deeper levels, below the intersection, the faults no longer offset horizons and deformation appears to be by folding alone. Depth conversion however reveals that apparent folding of the sub-thrust stratigraphy is due to velocity pull-up (see Brown, 1999) caused by the seafloor expression of the fold and the higher velocity rocks within the uplifted pop-up structure (Fig. 3a). Following conversion, stratigraphy below the branch point is planar (Fig. 3b) with a dip similar to the regional delta slope. Accurate description of the true deformation of this lower section is problematic due to poor imaging.

Cross sections are essential in clearly presenting the changing geometries, but 3D seismic data allow the along-strike transition from forethrust to backthrust to be resolved in greater detail. Fault sticks interpreted on successive diplines through this structure have been gridded to produce a 3D representation of the fault planes (Fig. 7d and e). The edges of the grids either correspond to the tip lines of the fault where displacement is zero, or the edge of the data set as labelled on the images. The figures do not show the entire grids, but only the portions near the fault linkage. The along-strike, horizontal overlap of the faults is approximately 3 km in this example. The upper tip-lines of both faults, shown as the top edges of the gridded surfaces, are located no more than 0.5 s (twt) under the seafloor. Tracing the tip-lines into the transfer zone there is a change in strike of the faults such that, at the tips, they curve as if to intersect each other (Fig. 5). This is similar to results from studies of fault segment linkage in extensional settings (e.g. Peacock and Sanderson, 1994). The shape of the lateral tip region of a fault plane is used in this study to define the geometry of fault interaction. The profile of a single fault and fold (Fig. 4) predicts isolated faults to be characterised by semi-ellipses (Fig. 8). Linked faults display modifications to this ideal that can be diagnostic of the type of linkage involved. In an antithetic Type 1 linkage faults have asymmetric, upward-tapering lateral tip regions (Fig. 8). This requires the lower tip lines to leave the zone of bed parallel shear in the detachment and climb stratigraphy towards relatively shallow lateral fault tips, while the upper tip lines maintain elevation. The result is an overlap of faults above the line of fault intersection, or 'branch line' (Boyer and Elliot, 1982; Butler, 1982; McClay, 1992), and an absence of faulting below this, close to

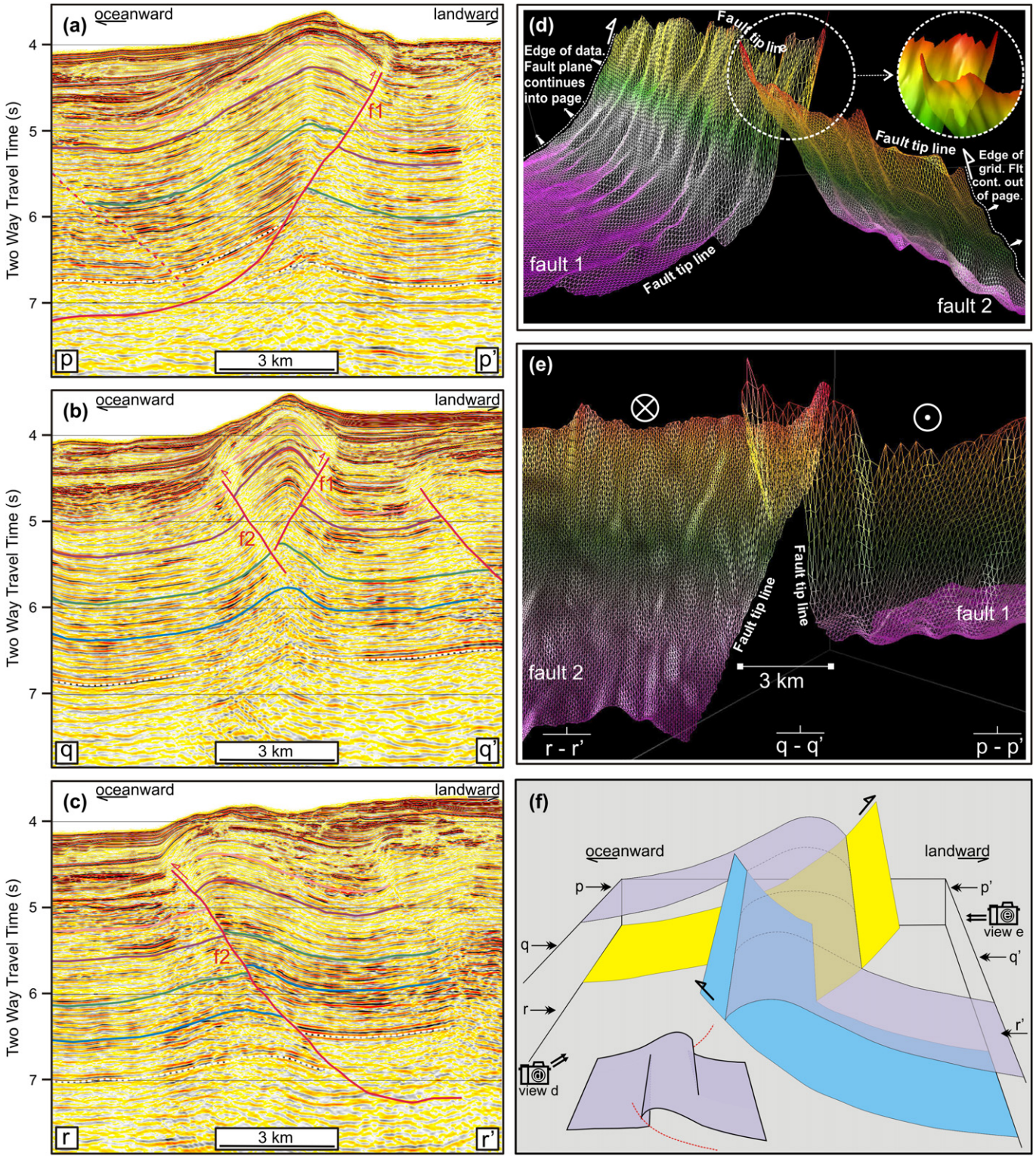

Fig. 7. Antithetic Type 1 linkage. (a,b,c) Downdip, sequential seismic sections in two-way-time (s). Fault 1 (f1) is a backthrust. Fault 2 (f2) is a forethrust. Agbada-Akata boundary: stippled white line. (d,e) 3D visualisations of fault planes using IESX Geoviz™ software. Surfaces are gridded from interpreted seismic fault sticks. Surfaces represent faults planes near the transfer zones only. Edges of the grids either represent fault tip lines (point of zero displacement) or the edge of the data set as labelled. In (e) a crossed circle indicates propagation into page; a dotted circle, propagation out of page. (f) Simplified block diagram of a Type 1 linkage. Yellow fault, backthrust; blue fault, forethrust. Transparent surface represents the hangingwall-hangingwall section of a typical shallow horizon. Inset surface shows increasing displacement along strike of typical shallow horizon away from the zone of fault overlap.

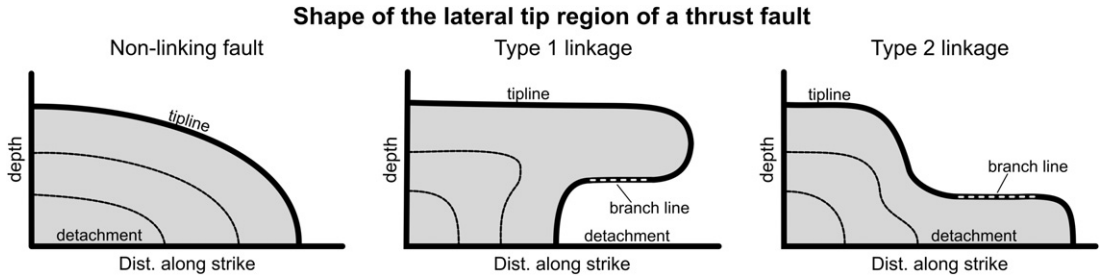

Fig. 8. Diagrammatical strike projections of faults to describe the shape of a fault plane around the region of the lateral tip for non-linking and linked faults. A non-linking fault describes a quarter-ellipse from d_{MAX} to tip (as here) and a semi-ellipse from tip to tip. A Type 1 linkage has an elevated lower tip line and an upward-tapering lateral tip region. A Type 2 linkage has a 'depressed' upper tip line and a downwards-tapering lateral tip region. Portions of tip lines that may form branch lines with counterpart faults (see Fig. 11) are indicated by white stippled lines. Type 3 is not shown as it does not have a diagnostic fault shape.

the detachment, within the transfer zone (Fig. 3b). This is best demonstrated in section (Fig. 7b) by contrasting the vertical extent of faulting relative to the branch point (Fig. 3b).

The geometry of this first class of linkage has been simplified in block form in Fig. 7f. An inset horizon has been included to demonstrate the increase in offset of horizons away from the zone of linkage. Stratal deformation varies with depth due to the shape of the lateral tip regions of the fault planes in the transfer zone. The horizon in Fig. 7f is at a relatively shallow level and is continuous and unbroken from hangingwall to hangingwall through the transfer zone.

4.2.2. Antithetic Type 2 linkage

An example of antithetic Type 2 linkage from this data set (Fig. 9) shows an along-strike reversal of thrust fault transport direction and fold vergence through the transfer zone, as in Type 1. The shape of the lateral tip region of the faults, however, and the geometry of the fault overlap is markedly different (Fig. 8). The fold associated with the thrust faults forms a continuous and buried anticline that trends obliquely to thrust strike through the centre of the transfer zone (Fig. 5b). Representative, successive seismic sections across this fold (Fig. 9a, b and c) give an illustration of this transition between forethrust and backthrust. In Fig. 9a a detaching backthrust carries a landward verging hangingwall anticline. The backlimb of this fold is onlapped by landward-stepping sedimentary packages. Maximum along-fault displacement on this fault is approximately 1.5 km. Footwall stratigraphy is essentially planar, but is deformed by a small forethrust (f2) with displacement of less than 200 m.

The structural geometry described in Fig. 9a is reversed on the other side of the transfer zone (Fig. 9c). In this instance the forethrust (f2) is dominant with approximately 1.3 km maximum along-fault displacement. Fold vergence is now oceanward with onlap packages, although present in the footwall, predominating in the hangingwall where they abut the long shallowly-dipping backlimb. Footwall deformation is characterised by a small backthrust with a maximum displacement of less than 200 m in this section.

A transfer zone lies between these two selected lines where neither forethrust nor backthrust is dominant (Fig. 9b). Maximum displacements are almost identical at 800 m and 900 m respectively. The two opposing thrusts are seen to abut, are over-steepened and underlie a 'bell-shaped' fold in the overburden. Changes to this structure during depth conversion were considered inconsequential. The symmetry of the fold and the vertical axial plane demonstrate a lack of vergence at this point and onlap packages occur on both limbs, stepping towards the anticlinal crest. This fold shape, with a lower interlimb angle, characterises Type 2 linkages within the dataset.

The wireframe and transparent fault planes (Fig. 9d, e and f) illustrate the forethrust and backthrust geometries in and around the transfer zone. The amount of along-strike overlap of these faults is calculated, by extrapolating fault displacement gradients for fault 2 beyond the data boundaries, as approximately 9.5 km. The switch in dominance of the corresponding faults, indicated by the amount of displacement and the height of the upper fault tip-line, occurs over a distance of 2 km. Unlike the Type 1 example, the trends of the fault planes in map view do not change strike into the zone of overlap despite a decrease in the elevation of the upper tip-line. Downward-tapering lateral tip regions (Fig. 8) lead to relatively deep lateral fault tips as the lower tip lines remain within a zone of bed parallel shear within the detachment. This causes faults to overlap exclusively below the branch point, seen in cross section (Fig. 9b), close to the detachment and results in an absence of faulting in the hangingwall above. Shallower horizons, those stratigraphically higher than the branch line, remain unbroken across the midpoint of the linkage zone (Fig. 9g, $q-q'$) due to displacement along a fault, and hence horizon offset, decreasing to zero at the tip lines and the shape of the lateral tip regions.

4.2.3. Antithetic Type 3 linkage

Linking faults need not be of similar displacement or lateral extent to form through-going folds. The antithetic Type 3 example (Figs. 6c and 10) comprises a backthrust measuring 9.5 km between lateral tips and a forethrust that extends 47 km from one lateral tip before being lost at the edge of the data set. Again, sequential seismic sections illustrate the changing fault geometries. In Fig, 10a a landward propagating backthrust (f1), detaching on the Agbada-Akata Fm boundary, produces a landward verging hangingwall anticline. An undisturbed seafloor suggests this fault is no longer active and depth conversion did not alter structural geometries to any significant degree.

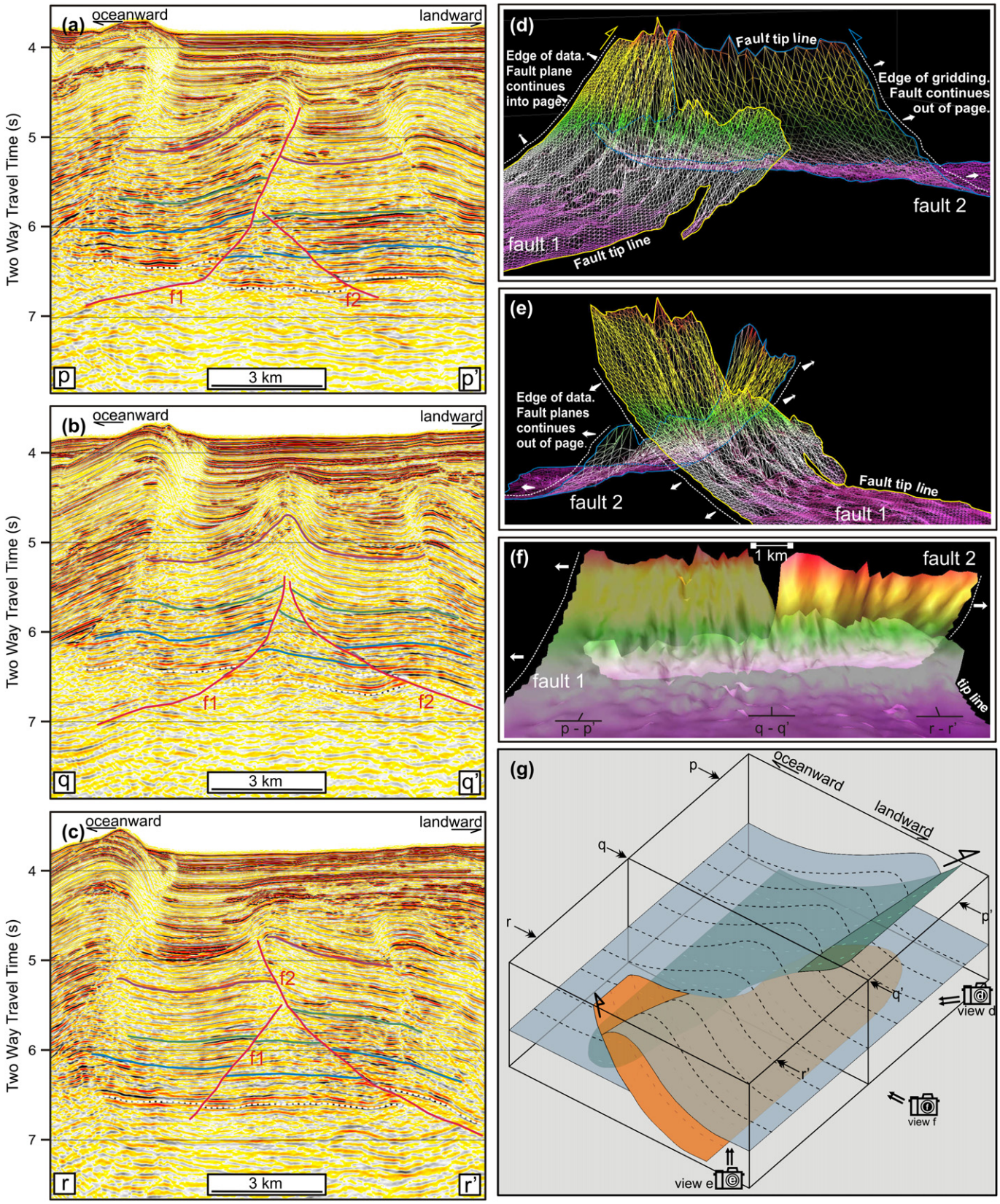

Fig. 9. Antithetic Type 2 linkage. (a,b,c) Downdip, sequential seismic cross-sections in two-way-time (s). Fault 1 (f1) is a backthrust. Fault 2 (f2) is a forethrust. Agbada-Akata horizon: stippled white line. (d,e,f) 3D visualisations of fault planes using IESX Geoviz™ software. Surfaces are gridded from interpreted seismic fault sticks. Surfaces represent fault planes near the transfer zones only. Edges of the grids either represent fault tip lines (point of zero displacement) or the edge of the data set as labelled. (g) Simplified block diagram of a Type 2 linkage. Green fault, forethrust; orange fault, backthrust. Transparent surface represents a typical shallow horizon.

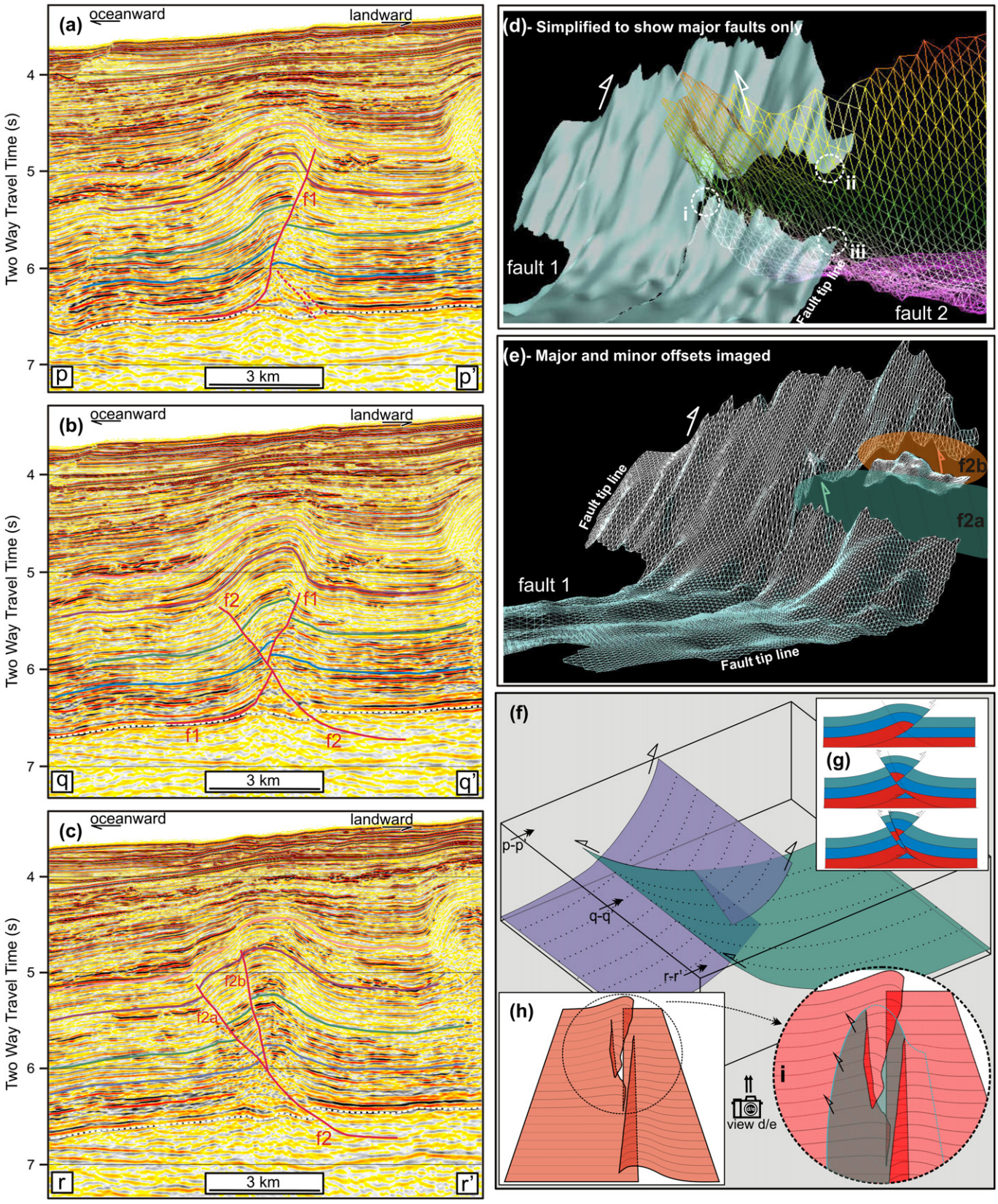

Fig. 10. Antithetic Type 3 linkage. (a,b,c) Downdip, sequential seismic cross-sections in two-way-time (s). Fault 1 (f1) is a backthrust. Fault 2 (f2a and b) is a forethrust. Agbada-Akata horizon: stippled white line. (d,e) 3D visualisations of fault planes using IESX Geoviz™ software. Surfaces are gridded from interpreted seismic fault sticks. Surfaces represent fault planes near the transfer zones only. Edges of the grids either represent fault tip lines (point of zero displacement) or the edge of the data set as labelled. In (d) fault 2 cross-cuts fault 1 displacing point (ii) from point (iii). (i) lies on the tip line of fault 2 and represents zero displacement along f2. In (e) idealised fault ellipses (f2a,f2b) represent the planes which cross-cut fault 1. (f) Simplified block diagram of a Type 3 linkage. Green fault, forethrust; blue fault, cross-cut backthrust. (g) Suggests a simple evolutionary history of fault linkage. (h) Stylised deformation of a horizon. An idealised fault semi-ellipse of f2 creates a new hangingwall (hw) anticline (right) whilst offsetting an existing hw anticline (left) producing a tapering, triangular section of stratigraphy.

Small, very low displacement forethrusts are present in the footwall and align with a slight bend in the backthrust fault plane. Displacement on the dominant backthrust is about 600 m here. Along strike (Fig. 10c), an oceanward verging fold overlies a forethrust (f2) that detaches within the Akata section. The shape of the fold is complicated by branching of the fault plane at around 6 s twt, possibly due to the formation of a footwall imbricate. This geometry is not spatially extensive and is only present for 2.5 km of the fold length close to the transfer zone. The footwall is relatively undeformed indicating this is outside the area of overlap.

Within the transfer zone (Fig. 10b) the backthrust (f1) is cross-cut by the less developed forethrust (f2), and complicated stratal geometries result along strike (Fig. 10 g and h). The complexity ensues due to the complimentary displacement patterns of faults 1 and 2 along strike (i.e. both faults are losing displacement towards the transfer zone). In Fig. 10d, 'i' represents a point of zero displacement on fault 2, whereas 'ii' and 'iii' locate two points of zero displacement on fault 1. Points 'ii' and 'iii' were once joined and have been separated by movement on fault 2. Fault 1 has therefore been cross-cut by fault 2. The crucial point to note therefore is that displacement *along* fault 1 decreases from the centre of its fault plane to the tipline, whilst the degree by which fault 1 is displaced when cross-cut increases in the same direction due to the interaction and nature of fault 2. This can lead to tapering, triangular sections of stratigraphy existing within the hangingwall-hangingwall section of the anticline (Fig. 10h). The fold retains a slight landward vergence within the transfer zone (Fig. 10b) due to the backthrust, at this point, having the larger displacement despite both faults acting upon the fold. The backthrust segment isolated within the forethrust hangingwall has convex-up curvature (Fig. 10b), suggesting deformation of the backthrust by folding prior to being cross-cut. The steady plunge of the fold across the transfer zone (Fig. 5c), the complimentary heave gradients and the cumulative heave curve similar to that of a single fold (Fig. 6) indicate these faults have been kinematically linked since conception (e.g. Nicol et al., 2002). The exclusive cross-cutting of fault 1 by fault 2, however, suggests fault 1 may have become inactive prior to the hard linkage of the faults.

The 3D model of the intersecting fault planes is more complicated than other types due to cross-cutting faults. The shape of lateral tip regions within the transfer zone (Fig. 10d) resemble that of non-linking faults (Fig. 8) with lower tiplines remaining in the detachment. The shape of the fault plane is therefore not distinctive for a Type 3 linkage and classification is based on both faults extending above and below branch lines in 3D, or the continuation of both faults past branch points in section, producing cross-cutting fault planes.

4.3. Comparing the structural geometry of transfer zones

The three types of antithetic fault linkage display very distinct fault plane geometries and fold styles within the transfer zones. The location and extent of faults relative to branch lines, and the offset and shape of selected horizons at various levels within the stratigraphy, are compared in Fig. 11.

The shape of the upward-tapering lateral tip regions of the faults in the Type 1 example leads to a 'pop-up' structure forming in the shallower section, such that neither fault reaches detachment within the zone of linkage. Hence, along the entire length of the related anticline there can be a maximum of one fault detaching into the shaly Akata Fm. In contrast to this, the anticlines associated with antithetic Types 2 and 3 linkages display double detachments within the transfer zones.

Horizon continuity across the folds, through the transfer zones, varies between the three types of linkage depending on the vertical extent of faulting relative to the branch lines (Fig. 11). Here, strata above this line are considered shallow and those beneath described as deep. In Type 1 the deeper horizons are continuous, planar and unbroken in a down-dip direction across the transfer zone, although a loss of seismic resolution in this area means smaller scale deformation may not be recorded here. Shallower horizons are also continuous along a convoluted surface through a hangingwall-hangingwall (hw-hw) transfer fold (Fig. 11). In contrast the deeper horizons in both the Type 2 and Type 3 geometries are connected through an indirect, undeformed footwall-footwall (fw-fw) 'corridor'. They differ within the shallow section however with the Type 2 horizons being continuous in a down-dip direction through the tight 'bellfold' whilst Type 3 horizons are connected by a tortuous hw-hw transfer fold (Fig. 11). Type 3 is more complex and horizons in the mid section, close to and above the convergence of the detaching thrusts, frequently show recurring repetition of stratigraphy.

5. Discussion

This is the first classification of antithetic thrust fault linkages and contributes to the understanding of fold and thrust belts. The three classes of forethrust–backthrust interaction are presented as static geometric observations. One of the major questions concerning how these geometries formed is whether folding predates fault growth and interaction, or whether fault interaction drives fold formation. Until this is determined, we cannot conclude the root causes of the different geometries, and therefore this contribution is descriptive. Several possible models could account for the structures seen in this study, for example:

1. Two kinematically separate faults with associated fault-propagation folds propagate laterally, converging and linking, creating a continuous fold (Fig. 12a).
2. Folding precedes faulting. In this case a laterally extensive fold forms first, then nucleating numerous faults along its length that grow by segment linkage; synthetic faults joining to form larger through-going faults, faults with opposing dip forming antithetic transfer zones (Fig. 12b).

Analogue models exist that support the second hypothesis, that folding precedes faulting (Dixon and Liu, 1991; Liu and Dixon, 1991). These authors suggest that numerous thrusts could nucleate at different points along a single fold and

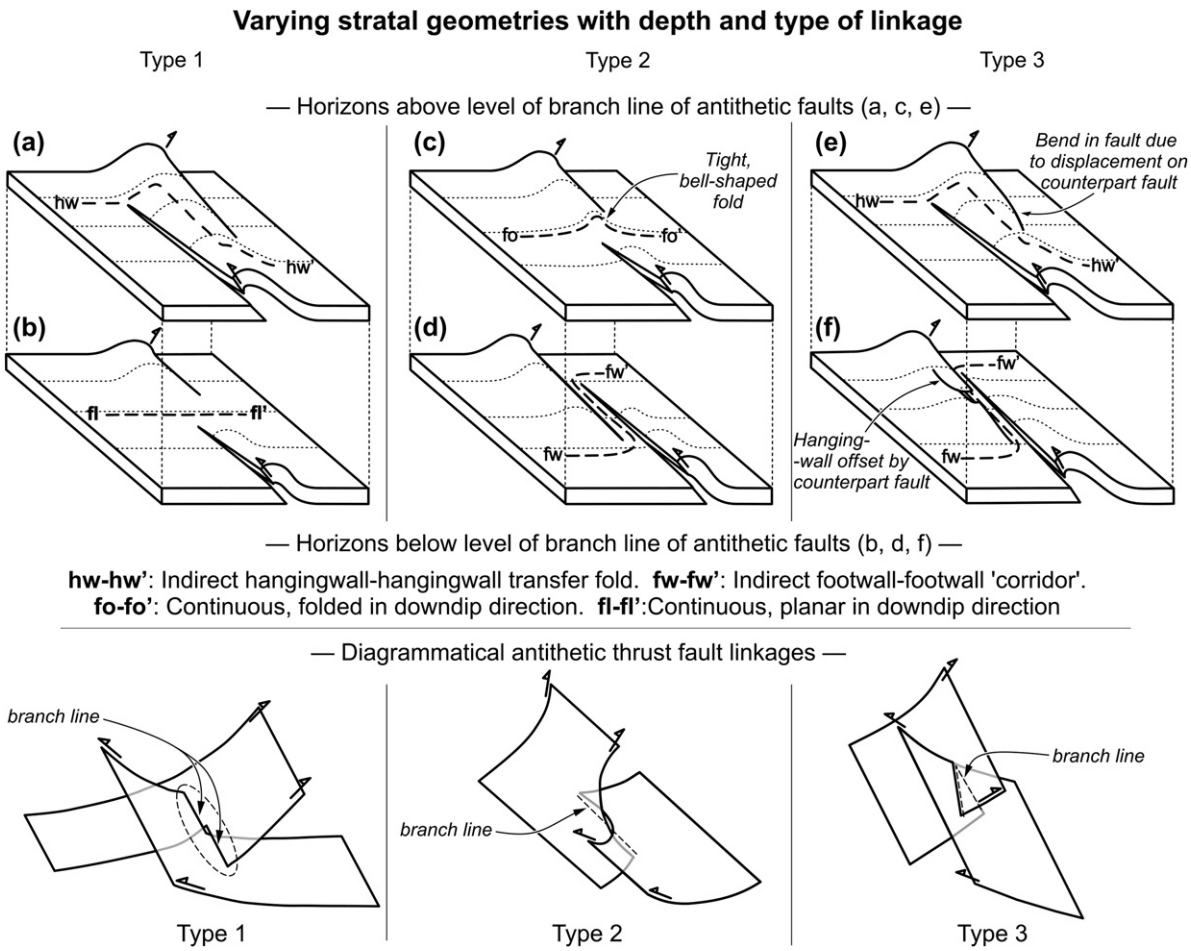

Fig. 11. Diagrammatical representation of the main stratal geometries of antithetic thrust fault relay zones. Two horizons are depicted for each linkage type, demonstrating the deformation above a branch line (a, c and e) and below (b, d and f). Simplified fault geometries are given to demonstrate the position of the branch lines.

propagate along strike, to link and produce larger structures. The models also show that the encompassing fold may be the product of along-strike propagation and linkage of several smaller, doubly plunging folds.

Few published examples of along-strike antithetic thrust linkage can be found within the literature: three are discussed here. Harrison and Bally (1988) describe the Parry Island Fold Belt, in the Canadian Arctic, as having a near equal development of forward- and backward-verging fold and thrusts. Numerous surface folds demonstrate along-strike vergence reversals (Harrison and Bally, 1988 their Figure 6) associated with apparent antithetic thrust fault linkage in the underlying succession (Harrison and Bally, 1988 their Figure 7). The authors describe ‘‘pop-up’’ structures within the transfer zones and relate them to displacement transfer between the overlapping thrusts. They create a model for ‘‘pop-up’’ formation that is similar in general to our Type 3 linkage (Harrison and Bally, 1988 their Figure 13).

Aamir and Siddiqui (2006) document an apparent Type 2 linkage between the Domeli Thrust (DT) and the Dil Jabba (DJ) Thrust in Eastern Potwar, Pakistan. In this study they show that the DJ thrust system overrides DT in the southwest whilst being overridden by DT, along strike, in the northeast. Between these two extremes they identify the point at which neither fault holds dominance (Aamir and Siddiqui, 2006 their Figure 16). This pattern suggests downward-tapering lateral tip regions indicative of a Type 2 linkage (Fig. 8), although fold styles in the overburden are not available for comparison. The DJ and DT faults result from northwest-southeast Himalayan compression (Aamir and Siddiqui, 2006) that creates a more complex thrust system than those in the Niger delta which are driven by gravitational collapse (e.g. Rowan et al., 2004). A Type 2 transfer zone present in a triangle zone of Eastern Potwar suggests that antithetic thrust fault linkages can be applied more generally than just to toe-of-slope fold and thrust belts.

Butler et al. (1987) describe alternating displacement between forethrusts and backthrusts in the Himalayan mountain front in the Salt Range of northern Pakistan. They discuss a necessary rotation of interacting thrust sheets of opposed polarity due to differing nature of forethrusts and backthrusts. They argue that the propagation of a backthrust may lead to the movement of the footwall ramp into the foreland due to footwall rocks being forced under the hangingwall. Forethrusts, on the

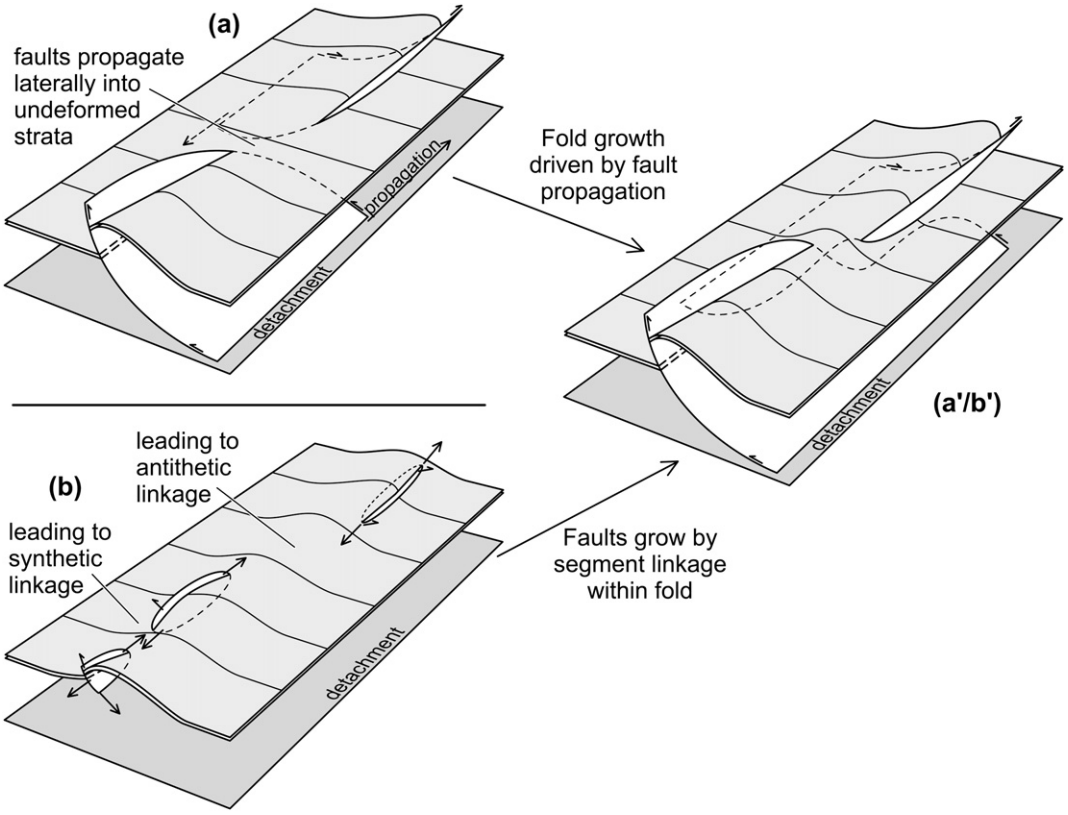

Fig. 12. Hypothetical models of the evolution of antithetic thrust fault linkage (based on a Type 2 linkage geometry). Two possible mechanisms of fold and fault linkage. (a) Two kinematically separate faults with associated fault-propagation folds propagate laterally, converging and linking, creating a continuous fold. (b) Folding precedes faulting. In this case a laterally extensive fold forms first, then nucleating numerous faults along its length that grow by segment linkage; synthetic faults joining to form larger through-going faults, faults with opposing dip forming antithetic transfer zones. (a′/b′) A schematic diagram of a Type 2 linkage observed in the data.

other hand, have static footwall ramps as hangingwall rocks are simply transported up and over the footwall (Butler et al., 1987). This was not observed in the fold and thrust belt of the Niger Delta, possibly due to lower fault displacements.

5.1. Implications

This research raises important questions about fault growth and linkage in compressional settings. Future work involving detailed displacement analyses and examination of fold and thrust timing may give clues to the controls on the type of linkage created at a point of fault interaction and the relationship between fault displacement and shortening within the transfer zones.

The geometry of three-dimensional thrust fault linkages described here could also impact modelling of fluid migration and transmissibility of deep water deltaic sequences. Understanding of (a) the connectivity of sand bodies in a stacked channel-levee system (b) the 3D geometry of the faults that intersect potential reservoir and seal lithologies and (c) how faults link the reservoirs to the underlying source rocks are all critical questions for successful hydrocarbon exploration and production.

6. Conclusions

We define three types of linkages of thrust faults of opposing dip within a fold and thrust belt.

Type 1. Faults overlap laterally within the shallow section only, above the level of the branch line of the antithetic thrusts. This creates a ‘pop-up’ structure within the transfer zone and a convoluted hangingwall-hangingwall (hw-hw) transfer fold.

Type 2. Faults overlap laterally within the deep section only, below the level of the branch line of the antithetic thrusts. This creates distinctive, tight folds in the overburden and an indirect, undeformed footwall-footwall (fw-fw) ‘corridor’.

Type 3. Faults cross-cut one another so that both are present above and below the branch line. Strata above this line form a convoluted hw-hw transfer fold, those below form an indirect, undeformed fw-fw ‘corridor’ with an increase in horizon repetition in the mid section.

All share the common feature of an along strike switch in vergence in the respective hangingwall anticline, however deformation of sediments within the transfer zones varies with

depth due to the shape of the lateral tip regions of fault planes as they overlap.

Such intersections represent a fundamental aspect of compressional fold and thrust belts and hence this simple scheme for defining how the component faults and folds link should have global applicability.

Acknowledgements

This study forms part of a PhD funded by Statoil at the 3DLab, Cardiff University, UK. We appreciate extensive discussion with Catherine Baudon and all at the 3DLab. This document was greatly improved by comments from Jonathan Imber, David Peacock, Rob Butler, Joe Cartwright, Richard Lisle and Paivi Heinio. We are grateful to CGG Veritas for the release of seismic data. We thank Schlumberger for the use of IESX software.

References

Aamir, A., Siddiqui, M., 2006. Interpretation and visualisation of thrust sheets in a triangle zone in eastern Potwar, Pakistan. The Leading Edge 25, 24–37.

Aydin, A., 1988. Discontinuities along thrust faults and the cleavage duplexes. In: Mitra, G., Wojtal, S. (Eds.), Geometries and mechanism of thrusting, with special reference to the Appalachians. Geological Society of America Special Paper 222, pp. 223–232.

Barnett, J.A.M., Mortimer, J., Rippon, J.H., Walsh, J.J., Watterson, J., 1987. Displacement geometry in the volume containing a single normal fault. AAPG Bulletin 71, 925–937.

Bilotti, F., Shaw, J., 2005. Deep-water Niger Delta fold and thrust belt modeled as a critical-taper wedge: The influence of elevated basal fluid pressure on structural styles. AAPG Bulletin 89, 1475–1491.

Boyer, S., Elliot, D., 1982. Thrust systems. AAPG Bulletin 66, 1196–1230.

Briggs, S.E., Davies, R.J., Cartwright, J.A., Morgan, R., 2006. Multiple detachment levels and their control on fold styles in the compressional domain of the deepwater west Niger Delta. Basin Research 18, 435–450.

Brown, A.R., 1999. Interpretation of Three-Dimensional Seismic Data. AAPG Memoir 42, SEG Investigations in Geophysics.

Butler, R., 1982. The terminology of structures in thrust belts. Journal of Structural Geology 4, 239–245.

Butler, R., Coward, M.P., Harwood, G.M., Knipe, R.J., 1987. Salt control on thrust geometry, structural style and gravitational collapse along the Himalayan mountain front in the Salt Range of northern Pakistan. In: Lerche, I., O'Brien, J.J. (Eds.), Dynamical Geology of Salt and Related Structures. Academic Press, Orlando, pp. 339–418.

Cartwright, J., Trudgill, B., Mansfield, C., 1995. Fault growth by segment linkage: an explanation for scatter in maximum displacement and trace length data from the Canyonlands Grabens of SE Utah. Journal of Structural Geology 17, 1319–1326.

Cartwright, J.A., Trudgill, B., 1994. Relay-ramp forms and normal-fault linkages, Canyonlands National Park, Utah. Geological Society of America Bulletin 106, 1143–1157.

Childs, C., Watterson, J., Walsh, J.J., 1995. Fault overlap zones within developing normal fault systems. Journal of the Geological Society, London. 152, 535–549.

Corredor, F., Shaw, J., Bilotti, F., 2005. Structural styles in the deep-water fold and thrust belts of the Niger Delta. AAPG Bulletin 89, 753–780.

Couzens, B.A., Wiltschko, D.V., 1996. The control of mechanical stratigraphy on the formation of triangle zones. Bulletin of Canadian Petroleum Geology 44, 165–179.

Dahlstrom, C.D.A., 1970. Structural Geology in the Eastern Margin of the Canadian Rocky Mountains. Bulletin of Canadian Petroleum Geology 18, 332–406.

Davis, K., Burbank, D.W., Fisher, D., Wallace, S., Nobes, D., 2005. Thrust-fault growth and segment linkage in the active Ostler fault zone, New Zealand. Journal of Structural Geology 27, 1528–1546.

Dawers, N., Anders, M., 1995. Displacement-length scaling and fault linkage. Journal of Structural Geology 17, 607–614.

Deptuck, M., Steffens, G., Barton, M., Pirmez, P., 2003. Architecture and evolution of upper fan channel-belts on the Niger Delta slope and in the Arabian Sea. Marine and Petroleum Geology 20, 649–676.

Dixon, D., Liu, S., 1991. Centrifuge modelling of the propagation of thrust faults. In: McClay, K. (Ed.), Thrust Tectonics. Chapman & Hall, London, pp. 53–70.

Douglas, R.J.W., 1958. Mount Head map area, Alberta: Canada. Geological Survey of Canada Memoirs 291, 241.

Doust, H., Omatsola, E., 1990. Niger Delta. In: Edwards, J., Santagrossi, P. (Eds.), Divergent/Passive Margin Basins. AAPG Memoir 48, pp. 201–238.

Eisenstadt, G., De Paor, D., 1987. Alternative model of thrust-fault propagation. Geology 15, 630–633.

Ellis, M., Dunlap, W., 1988. Displacement variation along thrust faults: implications for the development of large faults. Journal of Structural Geology 10, 183–192.

Gawthorpe, R.L., Hurst, J.M., 1993. Transfer zones in extensional basins: their structural style and influence on drainage development and stratigraphy. Journal of the Geological Society, London. 150, 1137–1152.

Harrison, J.C., Bally, A.W., 1988. Cross-sections of the Parry Islands Fold Belt on Melville Island, Canadian Arctic Islands: implications for the timing and kinematic history of some thin-skinned decollement systems. Bulletin of Canadian Petroleum Geology 36, 311–332.

Huggins, P., Watterson, J., Walsh, J.J., Childs, C., 1995. Relay zone geometry and displacement transfer between normal faults recorded in coal-mine plans. Journal of Structural Geology 17, 1741–1755.

Larsen, P.-H., 1988. Relay structures in the Lower Permian basement-involved extension system, East Greenland. Journal of Structural Geology 10, 3–8.

Liu, S., Dixon, D., 1991. Centrifuge modelling of thrust faulting: structural variation along strike in fold-thrust belts. Tectonophysics 188, 39–62.

Mandl, G., Crans, W., 1981. Gravitational gliding in deltas. In: McClay, K.R., Price, N.J. (Eds.), Thrust and Nappe Tectonics. Geological Society Special Publication, London. 9, pp. 41–54.

McClay, K.R., 1992. Glossary of thrust tectonics terms. In: McClay, K.R. (Ed.), Thrust Tectonics. Chapman & Hall, London, pp. 419–433.

Nicol, A., Watterson, J., Walsh, J.J., Childs, C., 1996. The shapes, major axis orientations and displacement patterns of fault surfaces. Journal of Structural Geology 18, 235–248.

Nicol, A., Gillespie, P., Childs, C., Walsh, J., 2002. Relay zones between mesoscopic thrust faults in layered sedimentary sequences. Journal of Structural Geology 24, 709–727.

Peacock, D.C.P., Sanderson, D.J., 1991. Displacements, segment linkage and relay ramps in normal fault zones. Journal of Structural Geology 13, 721–733.

Peacock, D.C.P., Sanderson, D.J., 1994. Geometry and Development of Relay Ramps in Normal Fault Systems. AAPG Bulletin 78, 147–165.

Peacock, D.C.P., Knipe, R.J., Sanderson, D.J., 2000. Glossary of normal faults. Journal of Structural Geology 22, 291–305.

Pfiffner, O.A., 1985. Displacements along thrust faults. Eclogae Geologica Helvetica 78, 313–333.

Rowan, M., Peel, F., Vendeville, B., 2004. Gravity-driven fold belts on passive margins. In: McClay, K. (Ed.), Thrust Tectonics and Hydrocarbon Systems: AAPG Memoir 82, pp. 157–182.

Segall, P., Pollard, D.D., 1980. Mechanics of discontinuous faults. Journal of Geophysical Research B 85, 4337–4350.

Suppe, J., 1985. Principles of Structural Geology. Prentice;Hall, Englewood Cliffs, NJ.

Walsh, J.J., Watterson, J., 1987. Distributions of cumulative displacement and seismic slip on a single normal fault surface. Journal of Structural Geology 9, 1039–1046.

Walsh, J.J., Watterson, J., 1991. Geometric and kinematic coherence and scale effects in normal fault systems. In: Roberts, A.M., Yielding, G., Freeman, B. (Eds.), The Geometry of Normal Faults. Geological Society Special Publication 56, pp. 193–203.

Watterson, J., 1986. Fault dimensions, displacements and growth. Pure and Applied Geophysics 124, 365–373.

Williams, G., Chapman, T., 1983. Strains developed in the hangingwalls of thrusts due to their slip/propagation rate: a dislocation model. Journal of Structural Geology 5, 563–571.